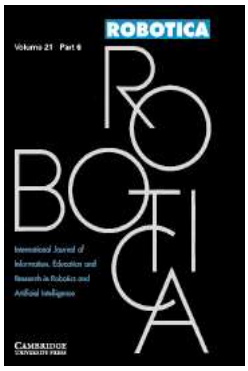

Design and control of a three degree of freedom pneumatic physiotherapy robot

R. Richardson, M. Brown, B. Bhakta and M.C. Levesley

Robotica / Volume 21 / Issue 06 / December 2003, pp 589 - 604
DOI: 10.1017/S0263574703005320, Published online: 24 October 2003

Robotica (2003) volume 21, pp. 589–604. © 2003 Cambridge University Press
DOI: 10.1017/S0263574703005320 Printed in the United Kingdom

Design and control of a three degree of freedom pneumatic physiotherapy robot

R. Richardson*, M. Brown‡, B. Bhakta† and M.C. Levesley*

(Received in Final Form: May 5, 2003)

SUMMARY

Stroke is a common condition resulting in 30,000 people per annum left with significant disability. In patients with severe arm paresis after stroke, functional recovery in the affected arm is poor. Inadequate intensity of treatment is cited as one factor accounting for the lack of arm recovery found in some studies. Given that physical therapy resource is limited, strategies to enhance the physiotherapists' efforts are needed. One approach is to use robotic techniques to augment movement therapy.

A three degree-of-freedom pneumatic robot has been developed to apply physiotherapy to the upper limb. The robot has been designed with a workspace encompassing the reach-retrieve range of the average male. Control experiments have applied force and then position only controllers to the pneumatic robot. These controllers are combined to form a position-based impedance control strategy on all degrees of freedom of the robot. The impedance controller performance was found to be dependent upon the specified impedance parameters. Initial experiments attaching the device to human subjects have indicated great potential for the device.

KEYWORDS: Impedance control; Pneumatic cylinders; Robotic physiotherapy.

NOMENCLATURE

x, y, z	= Displacement (m)
F_x, F_y, F_z	= Force respective to x, y and z (N)
V_x, V_y, V_z	= Voltages from force sensor (V)
C_Q	= Matrix of calibration coefficients
θ_1, θ_2, θ_3	= Angular displacement (rad)
K_{op}	= open-loop force control gain
M	= inertia
C	= damping (N/m^2)
K	= Stiffness (N/m)
x_d	= Position demand (m)
x_p, y_p, z_p	= global desired positions (m)
x_i, y_i, z_i	= Impedance trajectory (m)
θ_{1d}, θ_{2d}, θ_{3d}	= Joint space demands (rad)
τ_{ex1}, τ_{ex2}, τ_{ex3}	= torque on links due to external force

* Corresponding author. E-mail: rob@cs.man.ac.uk
Department of Computer Science, University of Manchester, Manchester M13 9PL (UK).
‡ WS Atkins Consultants Ltd, 220 Aztec West, Park Avenue, Bristol (UK).
† Rheumatology and Rehabilitation Research Unit, University of Leeds (UK).

1. INTRODUCTION

Stroke is a common condition (annual incidence 2 per 1000) and major cause of morbidity with 35% of patients left disabled.[1] Among those admitted with arm paresis, recovery in the arm is generally poor and has a major impact on self-care. A major component of arm rehabilitation after stroke is physical therapy. There is some evidence for a beneficial effect of physical therapy on recovery of the arm with a positive dose response relationship.[2,3] Even in rehabilitation services that purport to deliver an intensive program of physical therapy to patients with stroke, the amount of intervention may be inadequate because patients spend a large proportion of time not engaged in "rehabilitation" activities.[4] Given that physical therapy resource is severely limited, strategies to enhance the physiotherapist's efforts are needed. One approach is the use of robotic techniques to augment physical therapy.

Cozens[5] was the first to demonstrate responsive robotic assistance during an active patient arm exercise. Recently, prototype robotic devices have begun to be developed that have the potential to apply precise, quantifiable and repeatable movement therapy to stroke patients, however current prototypes tend to be complex and expensive.[6–8] The high power-to-weight ratio, low cost and direct drive capabilities of pneumatic actuators mean that the potential exists to make such devices simpler, and more affordable.

For a robot to administer physiotherapy it is connected directly to a human, whist considering both the force applied and its position. It is not possible to control force and position simultaneously, however several strategies for moderating force and position have been developed. The three main strategies are: hybrid force and position control, parallel force and position control, and impedance control. The hybrid force and position control strategy[9] controls force and position in orthogonal directions, enabling separate force and position controllers to be implemented on multi-degree-of-freedom systems. The parallel force and position control strategy[10] also controls the force and position in orthogonal directions but does not require predetermined knowledge of the environmental constraints. Both these controllers would behave solely as a force controller in this physiotherapy context due to contact always being maintained in all degrees of freedom between the robot and human. The impedance control strategy[11] does not control the position or force, but rather the dynamic relationship between the two. This enables a compromise between the two conflicting demands. The control aim is to change the manipulator end-point behaviour so its force and position relationship is given by a simple mass, spring and

damping arrangement. It has been shown that this strategy is appropriate for a robotic physiotherapy device.[6]

In any robotic device the actuators are normally the most significant component in terms of the device cost and effectiveness. Traditionally, pneumatic actuators were considered to be only useful for end stop positioning (fully extended or contracted). However, recent developments in pneumatic systems enable them to be considered for applications where previously only hydraulic systems or electric motors were suitable.[12–15] Few researchers have investigated force and position control strategies on pneumatic systems, mainly due to control difficulties caused by air compressibility. Impedance control applications, where low stiffness is required, can be difficult to implement on robots actuated by electric motors due to backlash and friction. In this instance, air compressibility is actually beneficial since it can enable smoother, more supple motion. Gorce and Guihard[16] have designed and simulated a multi-degree of freedom pneumatic impedance control strategy, where a pneumatic force model was used to control the force output of individual pneumatic cylinders. However, the difficulty of experimentally implementing accurate force control of pneumatic cylinders during motion should not be underestimated, with factors such as stiction and air compressibility combining to degrade the system performance. Indeed, Heinrichs et al.[17] found that an impedance controller based around position control was more appropriate during implementation on a hydraulic manipulator. Preliminary work on a single degree-of-freedom position-based impedance controller has demonstrated good results.[18] This paper extends this work to multiple degrees of freedom.

The remainder of the paper is structured as follows. Section 2 details the pneumatic components consisting of a 3 degree-of-freedom pneumatically actuated robot and simple three degree-of-freedom force sensor that measures the interaction forces. Section 3 demonstrates the performance of a PID controller implemented on one link of the pneumatic robot. Force control of the pneumatic cylinder is then investigated with both the position fixed and during piston movement. The combination of these force and position elements is then further developed, culminating in an impedance control strategy. The performance of this strategy is demonstrated on one degree of freedom on the pneumatic robot, and then extended to all three degrees of freedom of the prototype physiotherapy robot in the final part of Section 3. Section 4 assesses the suitability of the robot to implement physiotherapy. Discussion and conclusions are considered in Section 5.

2. EXPERIMENTAL APPARATUS

The experimental equipment consists of three parts: a three degree of freedom prototype physiotherapy robot; the pneumatic actuation system; and the three degree-of-freedom force sensor. An overview of all the system components is given in Table I.

2.1. The prototype physiotherapy robot

Conclusions drawn from design and development of single degree-of-freedom physiotherapy robot indicated that robotic physiotherapy has many potential benefits, however applications for single degree of freedom movement are limited.[19]

A three degree-of-freedom pneumatically actuated robot has therefore been designed and constructed (Figure 1) to take into account the optimum reach range of the average human. This can be approximated as the volume shown in Figure 2.[20] The robot has been designed so that its operational workspace encompasses this ‘optimum range’ of hand motions (Figure 3).

2.2. Pneumatic system

A pneumatic consisting of a low friction pneumatic cylinder and two electro-pneumatic valves actuation system provides the actuation force for the robot. The low friction cylinder minimises stiction effects enabling accurate control[14] and each valve supplies regulated pressure to a single chamber of the pneumatic cylinder (Figure 4). This enables the pressure difference across the cylinder to be specified by software changes alone and also allows the individual chamber pressures to be regulated by the valves themselves, avoiding the need for additional pressure control that has been implemented, for example, in reference [21]. To

Table I. Equipment specifications

Component	Properties
Low Friction pneumatic cylinder – Airpot Airpel – Air bearing design	Bore 0.627 inch Stroke: 6 inch
Electro-pneumatic pressure control valves – SMC E-P Hyreg VY1100	Pressure range: 0–8.8 bar Voltage Range: 1–5V
Force Transducer (three degree of freedom) Custom made	Capacity: 25 N all degrees of freedom
Force Transducer (single degree of freedom) RDP 51/1117-01	Capacity: 890 N Accuracy (%FS) ±0.5%
Linear rotary potentiometer Novotechnik P2701	Mechanical travel: 360° continuous Nominal resistance :5 kΩ
PC-Labcard PCL–727 12 channel D/A output card	12 D/A channels 12-bit resolution
PC-Labcard PCL 816/814B 16 A/D channels	16 A/D channels 16-bit resolution

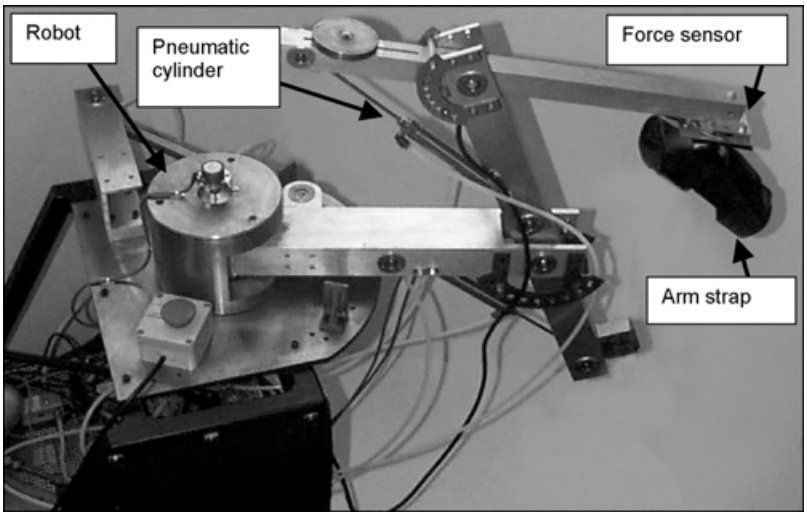

Fig. 1. Three degree-of-freedom pneumatic physiotherapy robot.

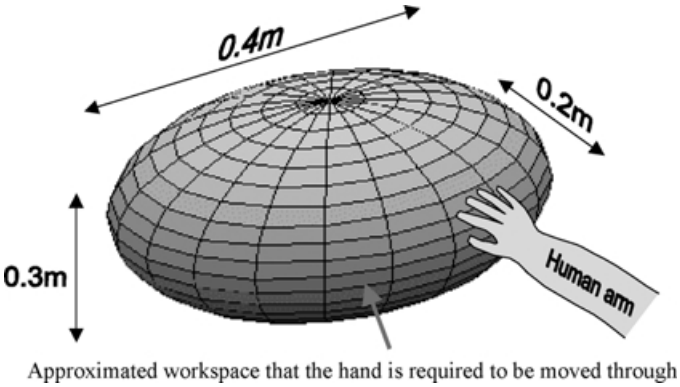

Fig. 2. Ergonomic operational range.

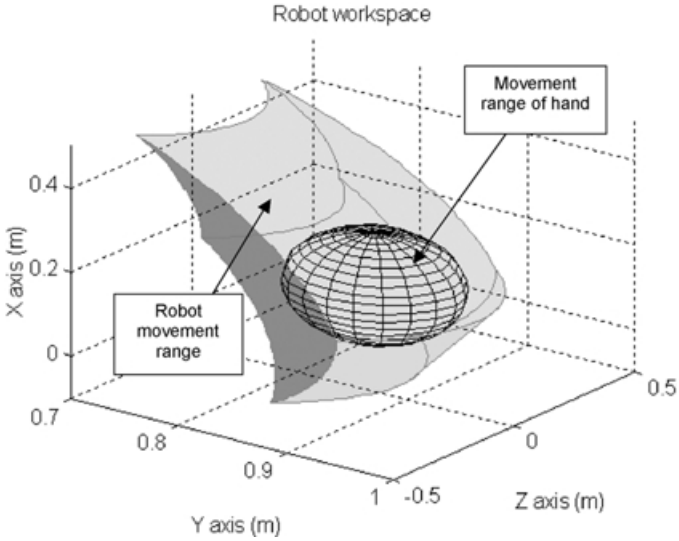

Fig. 3. Robot workspace.

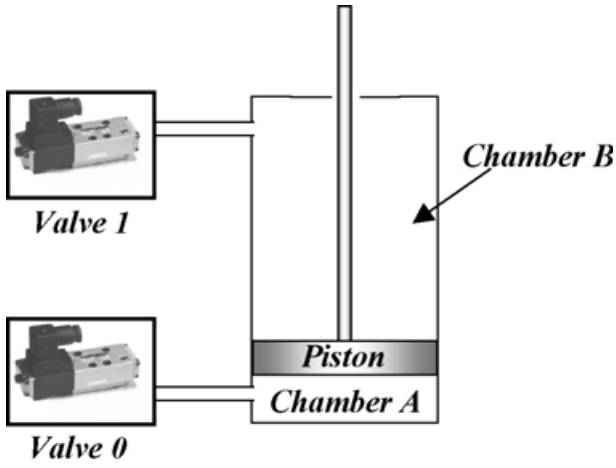

Fig. 4. The valve and cylinder arrangement.

achieve accurate control, it is desirable to control both valves from a single control signal. This has been achieved through the use of an equilibrium pressure for which one valve has pressure increased and the other valve has pressure decreased.[14] Thus, through manipulation of a single control voltage, the output force and, hence link position can be altered.

2.3. Force sensor

It is important to know the interaction forces between the robot and human at all times for two reasons: the interaction force needs to be monitored to ensure excessive forces are not applied to the human; and measurement of the applied force is required to implement the impedance control strategy. Commercial force sensors are available but can be overly expensive. In this paper, a simple three degree-of-freedom force sensor has been designed using finite element analysis techniques (FEA). Several other researchers have investigated the design of multiple degree of freedom force sensors. Kim et al.[22] designed and fabricated a six-degree of freedom force and moment sensor. Analysis of their design was performed using FEA and analytical techniques. The

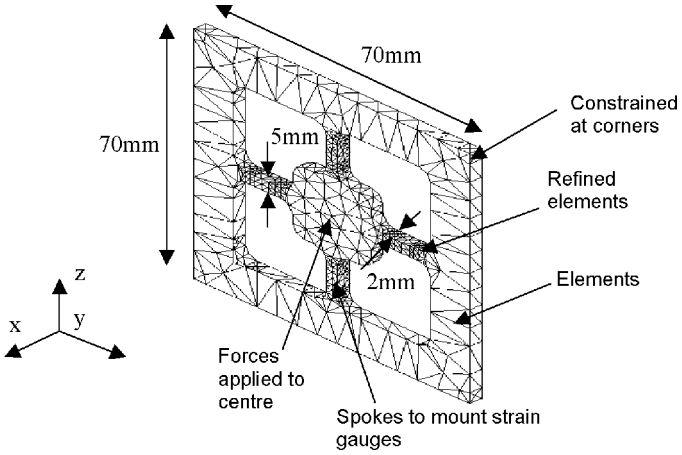

Fig. 5. Finite element representation of force sensor.

force/torque sensor was constructed using more than 50 strain gauges and was shown to be accurate, with little cross coupling of forces. Chao and Yin[23] designed a six component force and moment sensor for measuring the loading of human feet in locomotion. The force sensor was calibrated by collecting data while applying forces in single degrees of freedom. The sensor cross coupling was shown to be small. Both these designs operate well as multi-degree of freedom force sensors, however the complexity of the devices mean they are expensive to produce and require advanced manufacturing techniques.

2.3.1. Finite element sensor design. The force sensor used in this paper was designed based on a simplified version of Choa and Yin's[23] force and torque sensor. Design of the sensor was performed using FEA (finite element analysis) software. Finite element analysis provides a method of predicting the stress and strain within a component under specific loading conditions.[24] The finite element model constructed to develop the force sensor is shown in Figure 5. The mesh around the areas of interest (location of the strain gauges) is refined to contain smaller elements resulting in a more accurate prediction of strain gradients. The maximum required loading between the robot and force sensor was specified to be 20N.

The respective y and z FEA strain predictions when applying 20 N of force in the z direction is shown in Figure 6. Measurement of strain in the z direction requires strain gauges to be mounted on a spoke aligned with the z plane and strain in the y direction would be measured by placing strain gauges on a spoke in the y plane. Due to symmetry, strain predictions in the z direction, when rotated through 90°, will be valid predictions of the strain in the y direction. The FEA predications of strains produced by applying 20 N in the x direction are shown in Figure 7.

The finite element analysis demonstrates that by comparing the magnitude and respective phase of strain, forces can be measured in three degrees of freedom. The design of the force sensor allows two strain gauges to be attached to each spoke (one on each of the 5 mm spokes), allowing the use of

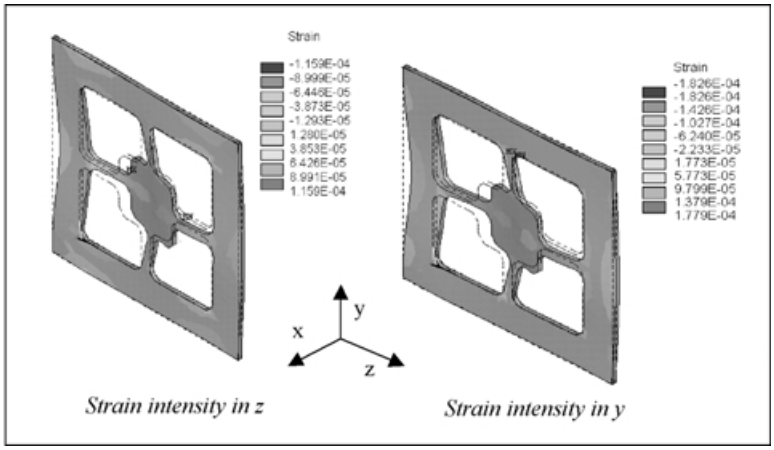

Fig. 6. Strain intensity for 20 N applied in z direction.

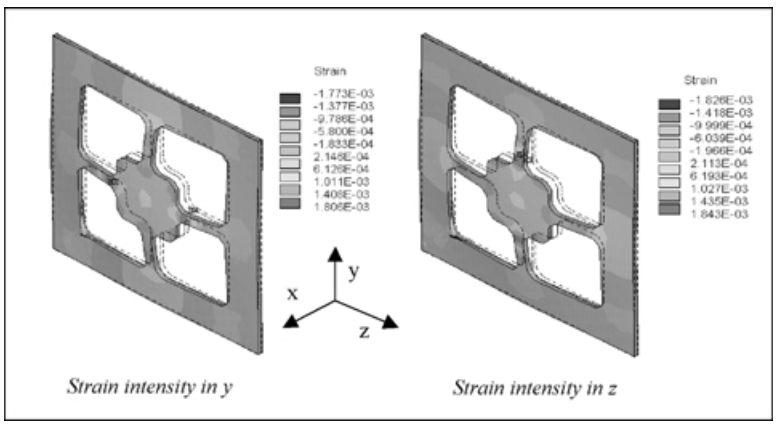

Fig. 7. Strain intensity for 20 N applied in x direction.

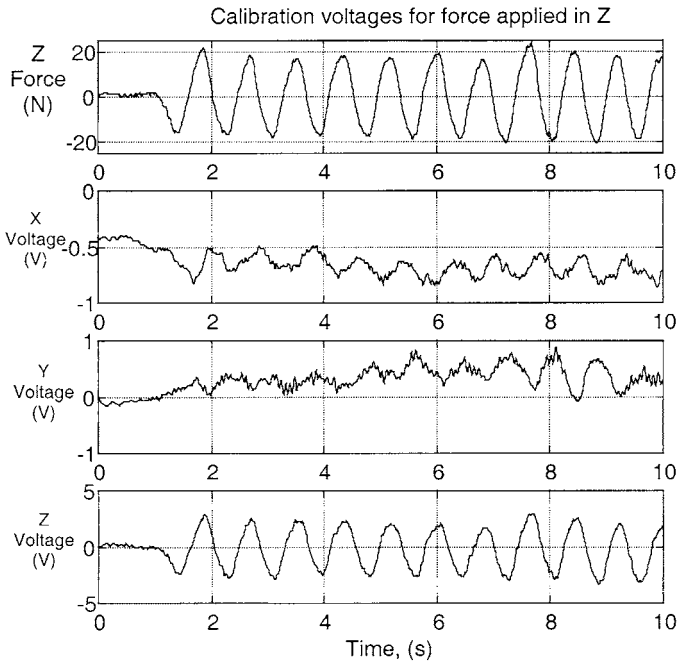

Fig. 8. Calibration voltages for forces applied in the Z direction.

eight strain gauges. One full wheatstone bridge was formed to measure forces in the x direction and two half wheatstone bridges measure the y and z forces. Each wheatstone bridge was attached to a separate strain gauge amplifier, resulting in three voltage outputs for any applied force. In the actual force sensor, external forces are applied to a spindle attached to the centre of the sensor. The sensor is secured in position by four bolts, one at each corner.

2.3.2. Calibration of the force sensor. Calibration of the force sensor voltages was required to reduce cross coupling and correlate measured voltages to applied forces. Ideally, to calibrate the force sensor, a commercial multiple degree-of-freedom force sensor would be useful. However, it is possible to use a commercial single degree-of-freedom force sensor to calibrate the sensor.[23] Three experiments, applying force in single degrees of freedom in the x, y and z plane were used to obtain calibration data.

The calibration voltages, when applying force in the z plane, are shown in Figure 8. The magnitude of the z voltage trace is significantly larger than the other directions indicating the sensor exhibits little inherent cross coupling. Combining the calibration data, enables a single calibration to be performed on the sensor.

Calibration of the force sensor using linear, bilinear, trilinear, and quadratic calibrations has been performed. In an ideal system a linear calibration would be most appropriate, however due to some non-linear aspects of the sensor the quadratic estimation provides the greatest accuracy.[25]

A quadratic estimate can also be used to calibrate the sensor as:

$$\begin{bmatrix} F_x \\ F_y \\ F_z \end{bmatrix} = [C_Q] \cdot [V_x \;\; V_y \;\; V_z \;\; V_x^2 \;\; V_y^2 \;\; V_z^2 \;\; 1]^T \qquad (2.1)$$

where C_Q is a matrix of quadratic calibration coefficients, estimated as:

$$[C_Q] = \begin{bmatrix} -8.51 & -1.03 & -0.28 & 0.98 & 0{,}27 & -0.57 & -3.19 \\ 1.30 & 5.53 & 0.21 & 0.21 & 0.23 & -0.28 & 0.23 \\ -0.43 & -0.45 & 7.126 & -0.26 & 0.09 & 0.13 & 1.11 \end{bmatrix} \qquad (2.2)$$

The results of this quadratic calibration are shown in Figure 9. Forces are applied to the sensor in three experiments, each applying forces to a separate degree of freedom. It is important to note that errors exist in the measurement of forces in all directions, but most importantly small forces are measured in directions where no force is applied. These false readings indicate that calibration has not completely removed coupling between directions, highlighting the non-ideality of the sensor solution.

3. ROBOT CONTROL

Control algorithms were applied to the robot to enable it to perform robot physiotherapy. These controllers were developed on a single degree-of-freedom of the robot (Figure 10). Angular rotation is measured by a potentiometer as θ_3, and force is measured at the robot endpoint by a force sensor aligned with the x plane. Initially, force control with the link position fixed was performed in Section (3.1). The force control experiments were repeated with the link free to move in Section (3.2) revealing dynamic elements to the force response. Position control of the individual links is performed in Section (3.3). The joint space position controllers and inverse kinematics enable global end-point positioning of the robot. The position controller and force controller are then combined in Section (3.4) to implement an impedance control strategy on a single link of the robot. This impedance control strategy is then implemented on a single degree of freedom in Section (3.5) and then all three degrees of freedom of the robot in Section (3.6).

3.1. Fixed position force control

Force only control can be applied to the single joint of the robot. Clamping the force sensor fixes the position of the link, preventing angular rotation. With the piston position fixed, the electro-pneumatic valves supply the pneumatic cylinder chambers (constant volume for fixed position) with air. The electro-pneumatic valves have within them analogue circuitry that regulates the output pressure to be proportional to input voltage. When the two valves are combined with a pneumatic cylinder, the voltage input to the pair can be considered proportional to the cylinder piston force output, thus enabling force control without feedback (open-loop control). Note that although open-loop demand signals are applied to the valve, the system cannot be considered completely open-loop due to analogue pressure regulation within the valves themselves. Figure 11 shows the force output and control signal for a square wave input and it can be seen the output force accurately tracks the desired.

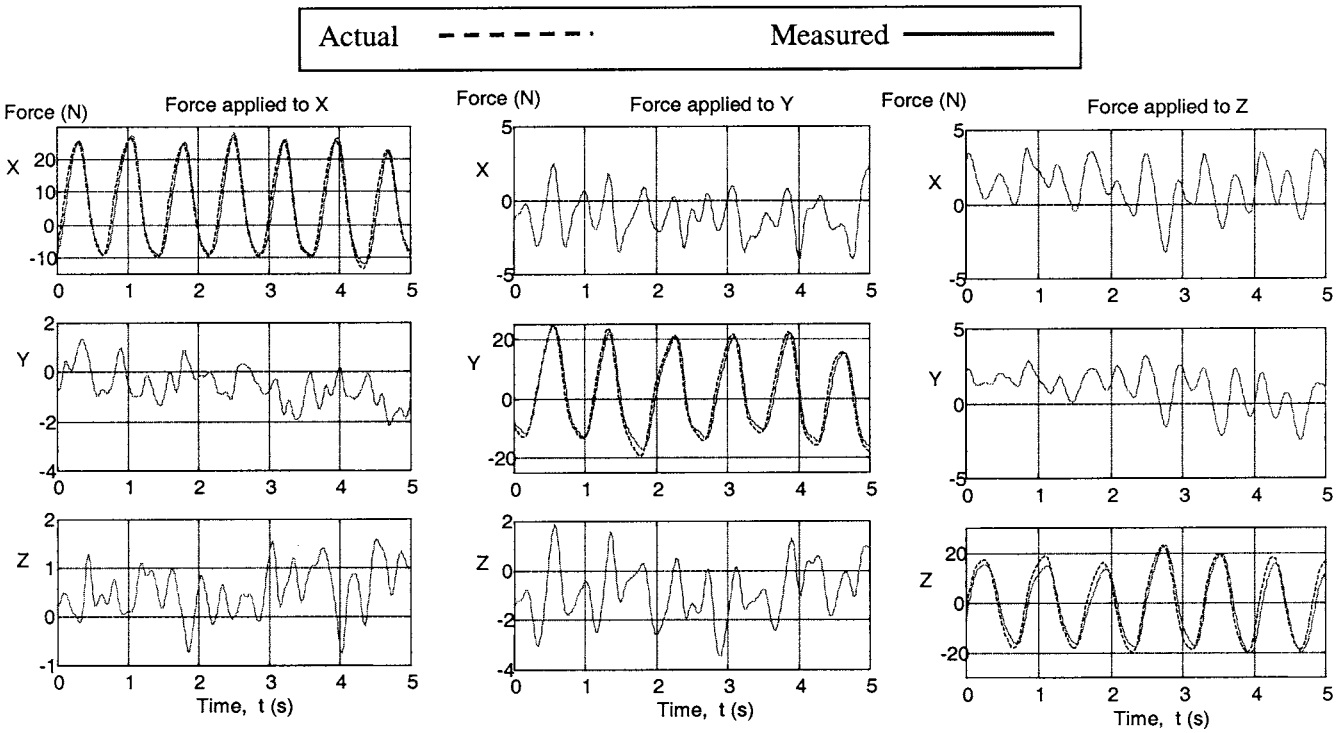

Fig. 9. Quadratic force calibration.

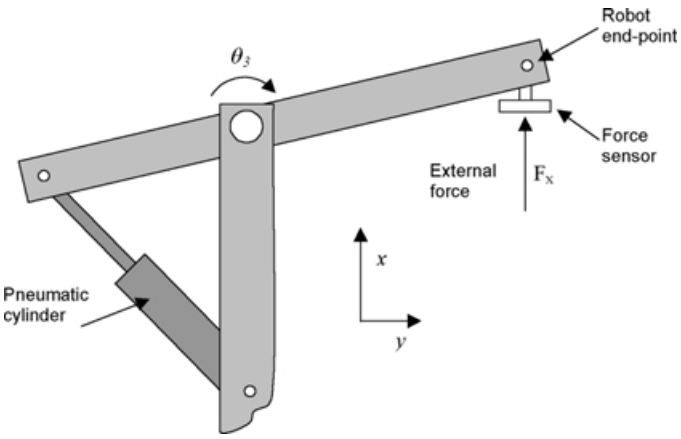

Fig. 10. Single joint of robot.

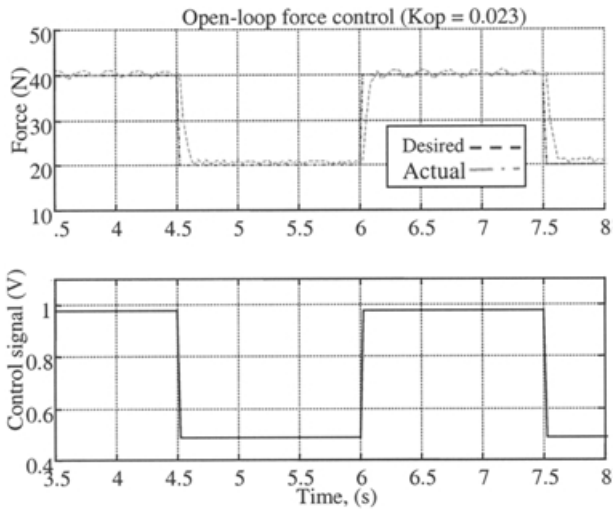

Fig. 11. Open loop force control.

3.2. *Force control*

Force control of the link can be performed when the force sensor is not clamped allowing the link to move. Ideally the open-loop force controller would apply a constant force regardless of link position. Indeed, the pressure regulation within the valves should achieve this. However, due to non-linear airflow dynamics and delays in response, the output force is affected by piston velocity. Figure 12 shows the force output of the pneumatic cylinder during motion for a sinusoidal input. The degradation of the force output during motion is important since it creates difficulties when implementing controllers that are based around force controllers.

3.3. *Position control*

Each joint of the robot requires separate position controllers which, when combined with inverse kinematics, enable global end-point positioning. Separate PID controllers were implemented to control the position of all three links of the robot. The PID gains for each joint controller were selected through an optimisation strategy. Methods of selecting the PID are well known for linear systems, such as the ultimate sensitivity method, however these are not necessarily ideal. Indeed pneumatic systems exhibit some non-linearity so experimentally optimising the controller performance ensures good performance. Using the downhill simplex method [26], the PID gains were optimised on-line using the ISTE criterion for quality of response [27]. Figure 13 shows the convergence of the PID controller parameters for the third link. The optimised PID step response is shown in Figure 14. The identified PID gains for each joint are shown in Table II.

The optimised PID joint space controllers and inverse kinematics enable global positioning of the robot end-point

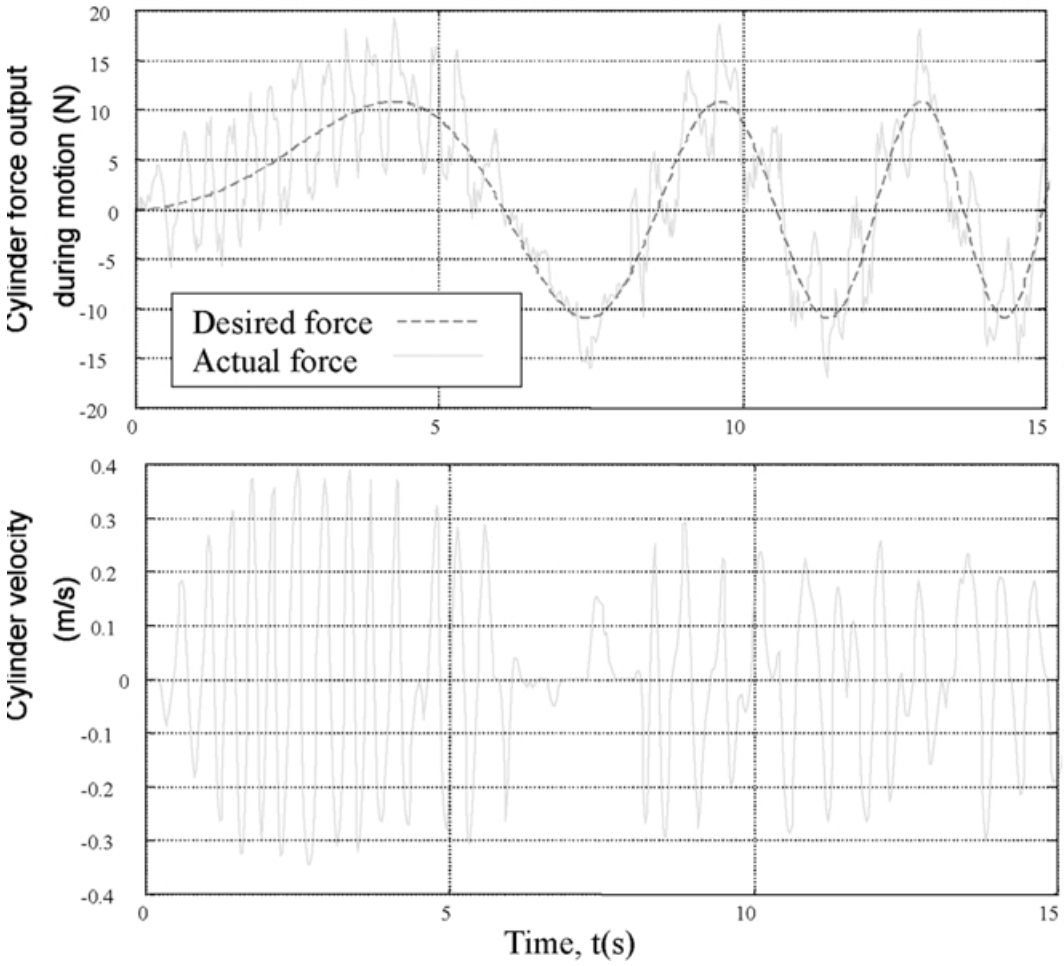

Fig. 12. Cylinder force output during motion.

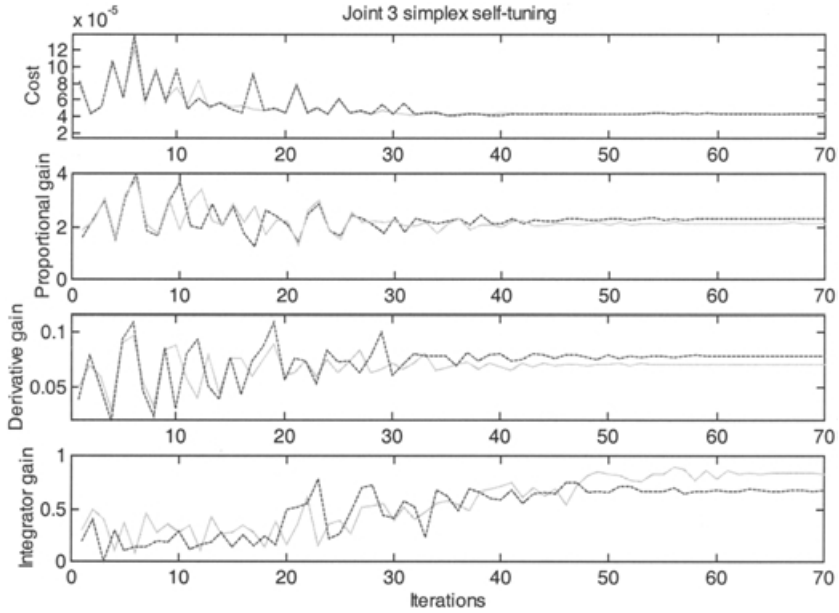

Fig. 13. Convergence of joint 3 PID parameters.

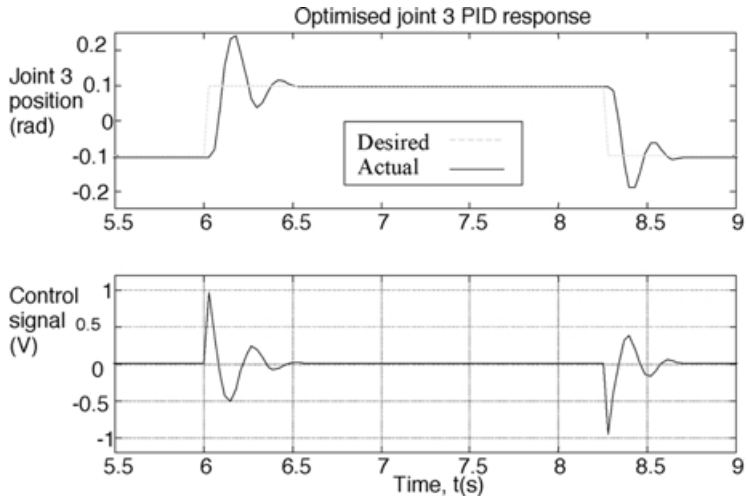

Fig. 14. Optimised joint 3 PID response.

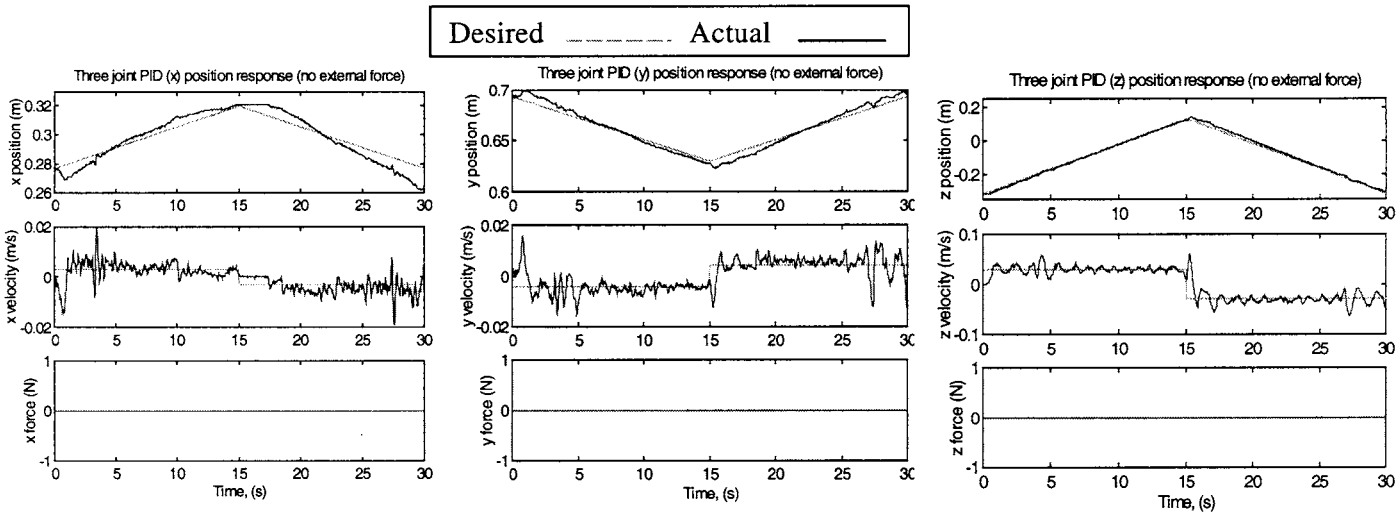

Fig. 15. Three degree-of-freedom position response.

Table II. Optimised controller gains

	Proportional (P)	Derivative (D)	Integral (I)
Joint 1	18	2.5	0.04
Joint 2	5.5	0.45	0.5
Joint 3	2.2	0.065	0.7

in three degrees of freedom. Figure 15 shows the position response in three degrees of freedom to a ramp input with slow change (the low desired velocity of the pneumatic system makes it easier to detect stiction and is realistic of the final robot motion). The desired position is tracked, however the motion is not perfectly smooth as indicated by the error in the velocity response.

3.4. Impedance control

Impedance control has been developed over the last decade to enable robots to smoothly move between contact and non-contact phases of motion. Examining how humans interact with their environment was an integral part of this development. Impedance control fixes the relationship between the manipulator end-point and external disturbances. In position-based impedance control, the impedance controller alters the position for any force applied to the robot end-point.

Impedance control utilises a mass, spring and damper relationship between force and position (Figure 16). The transfer function connecting force and position used in position-based impedance control (admittance control), can be specified in the s-domain as:

$$\frac{x_i}{F_x} = \frac{1}{Ms^2 + Cs + K} \tag{3.1}$$

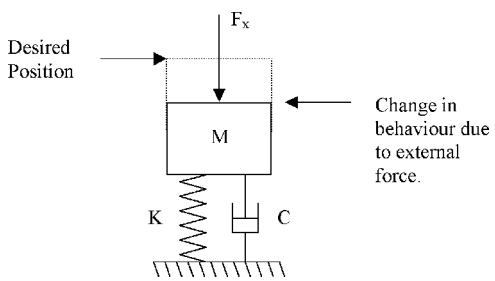

Fig. 16. Impedance control free body diagram.

where x_i is the change in position due to external force (F_x), M is the inertial component, C is the damping component and K is the stiffness component.

Rearranging Equation (3.1) so that position becomes the input, known as force-based impedance control gives:

$$\frac{F_x}{x_i} = Ms^2 + Cs + K \tag{3.2}$$

Equations (3.1) and (3.2) are known as the duality of impedance control. These two subtly different approaches require different controller structures. A more detailed discussion of these differences can be found in reference [25], but a summary of the advantages and disadvantages of each type of impedance controller is given in Table III. As highlighted by [17], position-based impedance control (admittance control) is more appropriate for pneumatic systems.

The position controller described earlier is not robust to external forces. However, it was demonstrated in the force control section that open-loop force control is effective for fixed position force control. Combining the position controller and open-loop force controller greatly increases the controller's ability to reject force disturbances. The overall impedance control strategy is shown in Figure 17 (for a single link).

3.4.1. Single degree-of-freedom impedance control. The impedance controller has been applied to a single joint of the robot. The external forces are measured through the force sensor mounted at the manipulator end-point (Figure 10). Note it is in fact the force error that causes a change in set-point, however, in this particular situation the desired force is zero, therefore, the external force itself becomes the force error.

The resulting demand for the position controller (x_d) becomes

$$x_d = x_i + x_p \tag{3.3}$$

where x_p = desired position without any external forces

In order to evaluate the controller performance in the single link of the robot, a mass was attached and removed from the robot end-point while the robot's desired position was constant ($x_p = 0$). With the mass attached, an approximately constant force was applied to the robot end-point. This is not representative of disturbances in the physiotherapy context, but rather an extreme test of controller performance.

The results obtained with inertia, damping and stiffness (Figure 18), show that the end-point closely follows the desired trajectory. For small oscillations the experimental tracking is poor, mainly due to friction within the system. Examining the voltage output from the position controller and open-loop force controller (Figure 19) illustrates the operation of each element of the impedance controller. The open-loop force controller provides a compensation force to oppose link movement due to the external force. The position controller's output moves the link along the desired trajectory providing little compensation for the external force, as such its output is much smaller than the force controller. The performance of the position controller is sufficient to compensate for the open-loop force controller error experienced during motion.

Although impedance control can be performed with inertia, damping and stiffness, the inertial element is

Table III. Comparison of Admittance control and impedance control

	Admittance control	Impedance control
Advantages	• Most appropriate for environments consisting of stiffness and damping elements [28]. • Only requires addition of a force sensor on conventional robotic devices based around measurement of link position..	• Most appropriate for environments consisting of inertial element [28]. • Easy to implement on direct-drive electric motor systems due to the ease at which torque can be controlled during motion.
Disadvantages	• Requires a high gain position controller robust to external force disturbances	• Difficult to implement on actuator systems where force output is effected by robot movement. • Requires robot inertial model, which can be difficult to obtain.

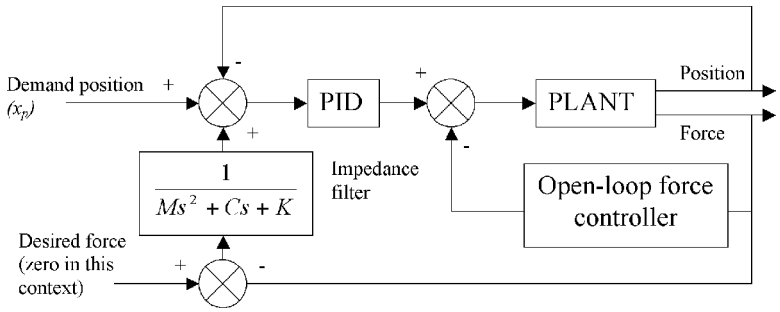

Fig. 17. Impedance controller block diagram.

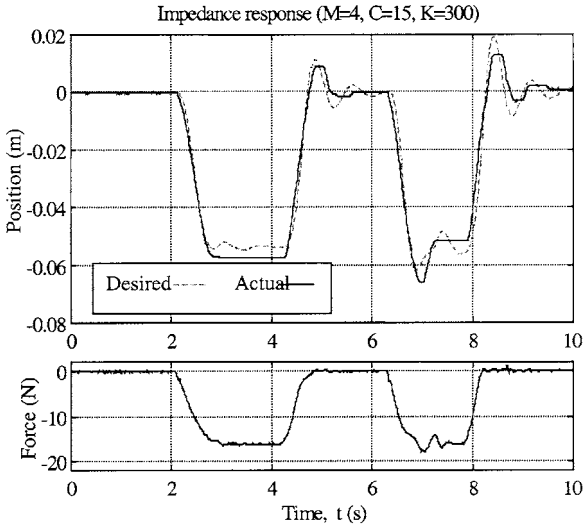

Fig. 18. Single degree-of-freedom impedance controller result (M=4,C=15,K=300).

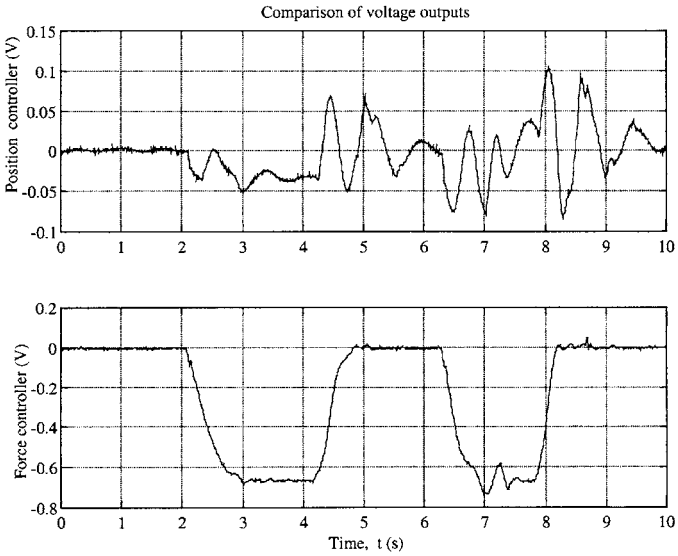

Fig. 19. Voltage outputs for response (M=4, C=15, K=30).

considered to offer little therapeutic value for physiotherapy [6]. Damping and stiffness alone can be specified for impedance control, requiring the controller to mask the physical inertia within the link. Examining the results obtained with only damping and stiffness (Figure 20), shows that the endpoint accurately tracks the desired trajectory. Some steady state offset is present within the system due to modelling errors when resolving forces.

The impedance controller can be implemented in multiple degrees of freedom, and this is illustrated in the next section.

3.4.2. Multiple degree-of-freedom impedance control. A flow chart of the multiple degree-of-freedom controller is shown in Figure 21. The desired end point trajectory is specified before implementing the controller, in the form of

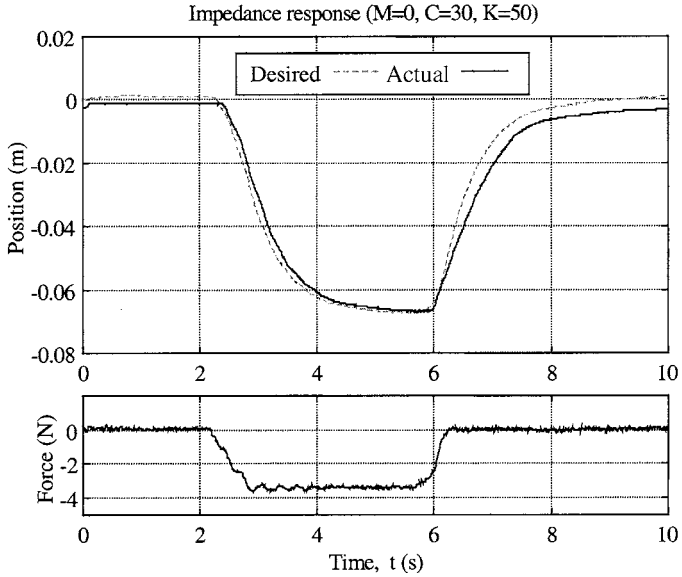

Fig. 20. Single degree-of-freedom impedance control (M=0, C=30, K=50).

global position co-ordinates (x_p, y_p, z_p). These co-ordinates, when added to the desired change in position due to external forces (as a result of the impedance filter) (x_i, y_i, z_i), form the desired robot position at any instant. The desired global positions are converted into joint space demands (θ_{1d}, θ_{2d}, θ_{3d}), using the robot inverse kinematics. Three independent controllers implement the desired joint space positions.

External forces are resolved through the robot to obtain their influence on each joint (τ_{ex1}, τ_{ex2}, τ_{ex3}). An equal, but opposite force is generated by the joint space open-loop force controllers, to reduce the effects of these external forces on link position.

The forward kinematics of the joint positions reveal the robot end position in task space co-ordinates (x, y, z). External forces are measured at the robot end-point using the three degree-of-freedom force sensor. Three separate impedance filters convert the global external forces F_x, F_y and F_z into changes of the x, y and z desired task space co-ordinates respectively. Note that it is possible to implement different impedance filters for different degrees of freedom enabling one degree of freedom to be stiff while another is compliant.

The impedance controller with damping and stiffness has been experimentally implemented on all three degrees of the pneumatic robot. To assess the controller performance, five alternative stiffness and damping parameters were assessed. Due to the inertia of the robot links and delays in the robot response it is not possible to implement zero damping and stiffness (this would result in zero force for any movement of the robot end-point). A stiffness value of 50 N/m and damping of 50 N/ms represents the approximate minimum values (test 1). Test 2 increases the stiffness to 170 N/m while maintaining damping at 50 N/ms. This assesses the performance of increased stiffness that would be used in a physiotherapy context, to increase the force towards the desired trajectory if the patient was experiencing difficulty.

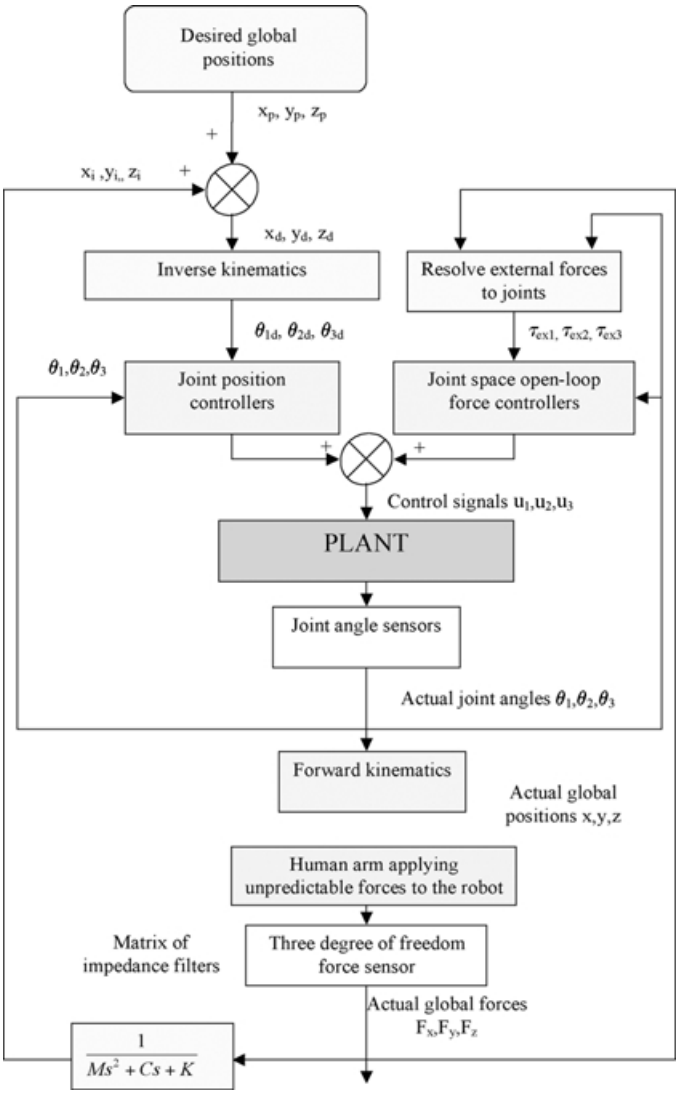

Fig. 21. Implementing impedance control in multiple degrees of freedom.

Test 3 implements a stiffness of 50 N/m with damping of 170 N/ms. The increased damping here could be used to reduce tremor that may be present in a patients motion. Test 4 increases the stiffness to 250 N/m and damping to 250 N/ms. This is designed to be an extreme test of controller performance with large forces resulting in little displacement. These are likely to be the largest values use due to the strength and weight of the human arm combined with the motion of the robot. Finally test 5 implements a stiffness of 130 N/m and a damping of 130 N/ms to test the controller performance at around the middle of the available stiffness and damping parameters. For all of these experiments a circular force crossing the x, y and z axes was applied by a human subject, resulting in sinusoidal forces in the x, y and z direction. Below is a summary of the performance of each test.

Test 1: K = 50, C = 50 (Figure 22)
Sinusoidal forces of ±8 N are applied to the robot end-point while it y and z plane while x remains constant. A small delay is present in the x position response, combined with slight error in the magnitude of the response. The velocity of the x plane is also accurately tracked. The x and y responses are accurately tracked.

Test 2: K = 170, C = 50 (Figure 23)
Approximate sinusoidal forces of ±8 N are applied in x, y and z to the robot end-point while it extends and retracts in the y and z-plane. For large movements the motion is accurately tracked, however the required motion for small forces is not achieved. This is likely to be due to errors in force measurement as the multiple axis force sensor has been shown to be susceptible to input torque.

Test 3: K = 50, C = 170 (Figure 24)
Sinusoidal forces of ±12 N are applied in x, y and z to the robot end-point while it extends and retracts in the y and z-plane. Due to the increased damping the number of force

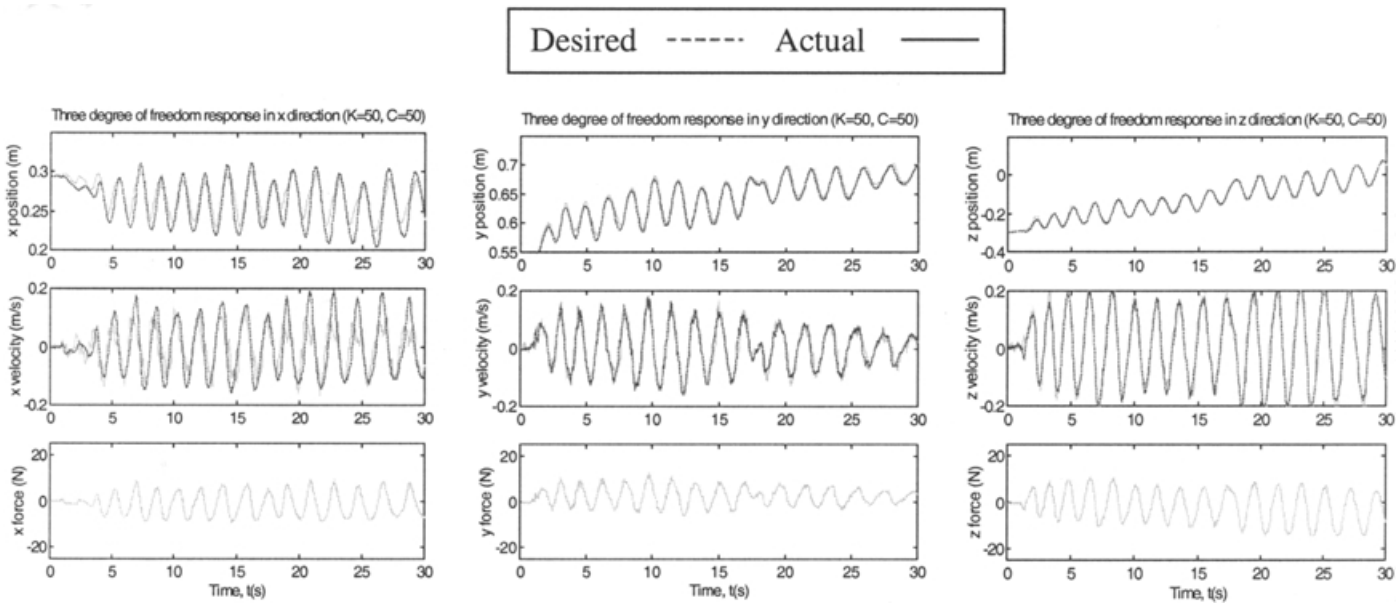

Fig. 22. Three degree-of-freedom impedance controller response (K = 50, C = 50).

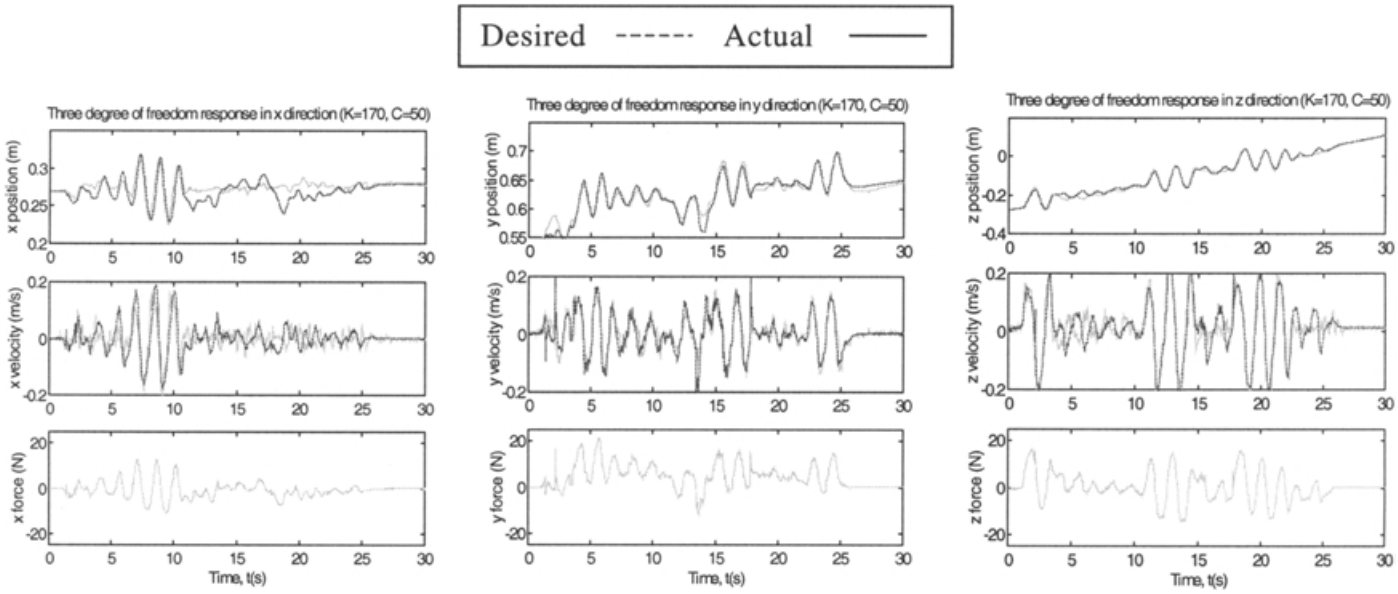

Fig. 23. Three degree-of-freedom impedance controller response (K = 170, C = 50).

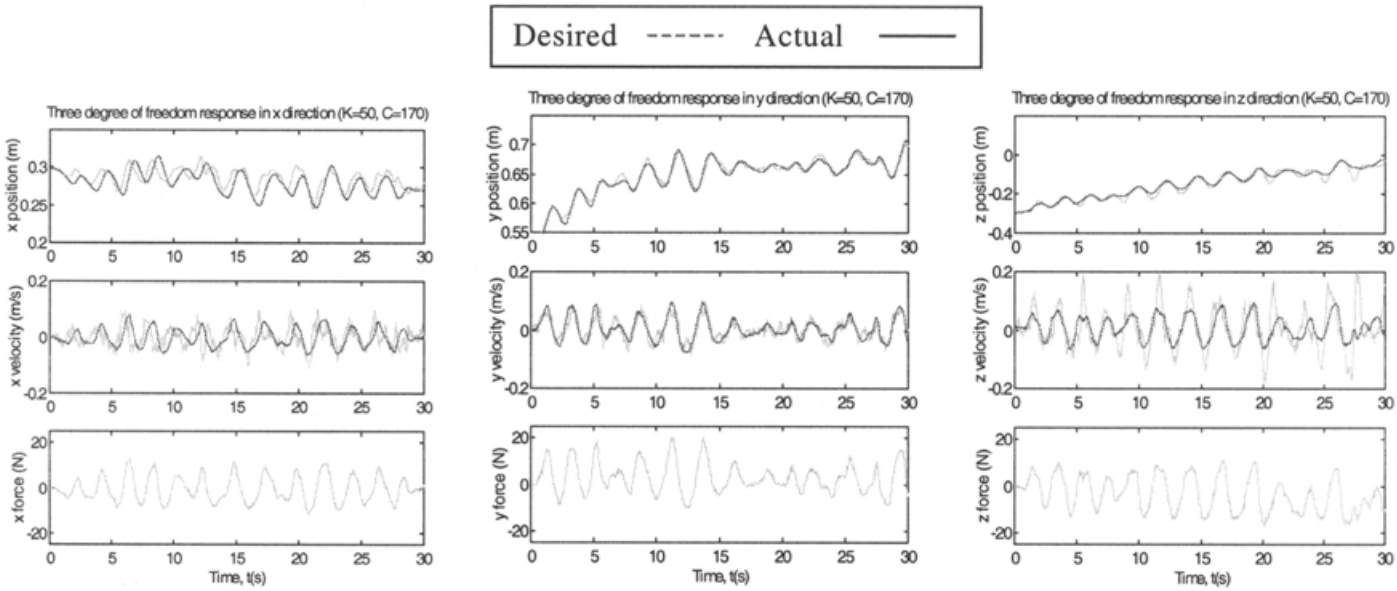

Fig. 24. Three degree-of-freedom impedance controller response (K = 50, C = 170).

cycles the subject has applied to the robot end-position has decreased. The increased damping results in a poorer response in all three axes.

Test 4: K = 250, C = 250 (Figure 25)
Increasing the stiffness and damping results in the subject experiencing difficulty applying external forces to the robot end-point which are large enough to assess the controller performance. Due to this approximate sinusoidal forces of ±15 N were applied in the x, y and z-plane. This represents the most extreme test of controller performance with the controller required to accurately control the position while balancing these external forces. The x and z motions are poorly tracked. This is especially apparent in the velocity response. The poor quality of the response is due to the magnitude of the applied forces and the susceptibility of the force sensor misread torque as force.

Task 5: K = 130, C = 130 (Figure 26)
Sinusoidal forces of ±14 N are applied in x and y to the robot end-point. The reduction in the stiffness and damping parameters from task 4 enables an improvement in the sinusoidal input force. The position tracking is worse than that of task 1 due to the increased input forces. However the x, y and z responses have approximately the correct magnitude and shape.

The results show the robot capable of implementing an impedance control strategy with varying stiffness and damping parameters. It is important to note that the impedance control strategy does not offer consistent

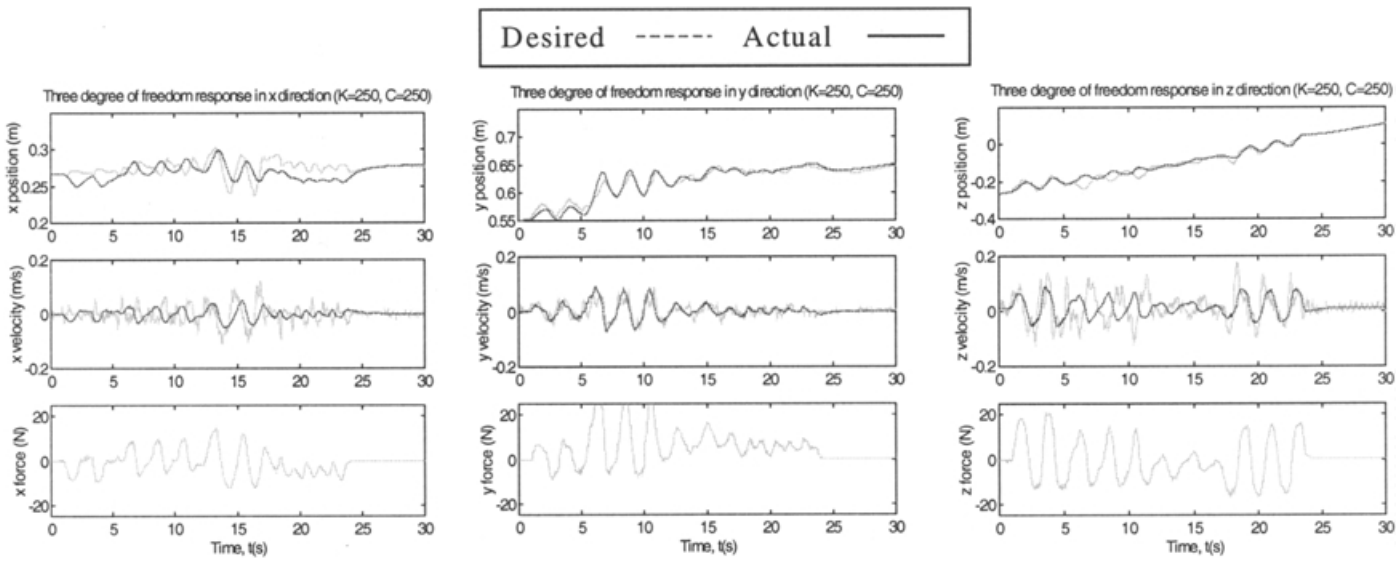

Fig. 25. Three degree-of-freedom impedance controller response (K = 250, C = 250).

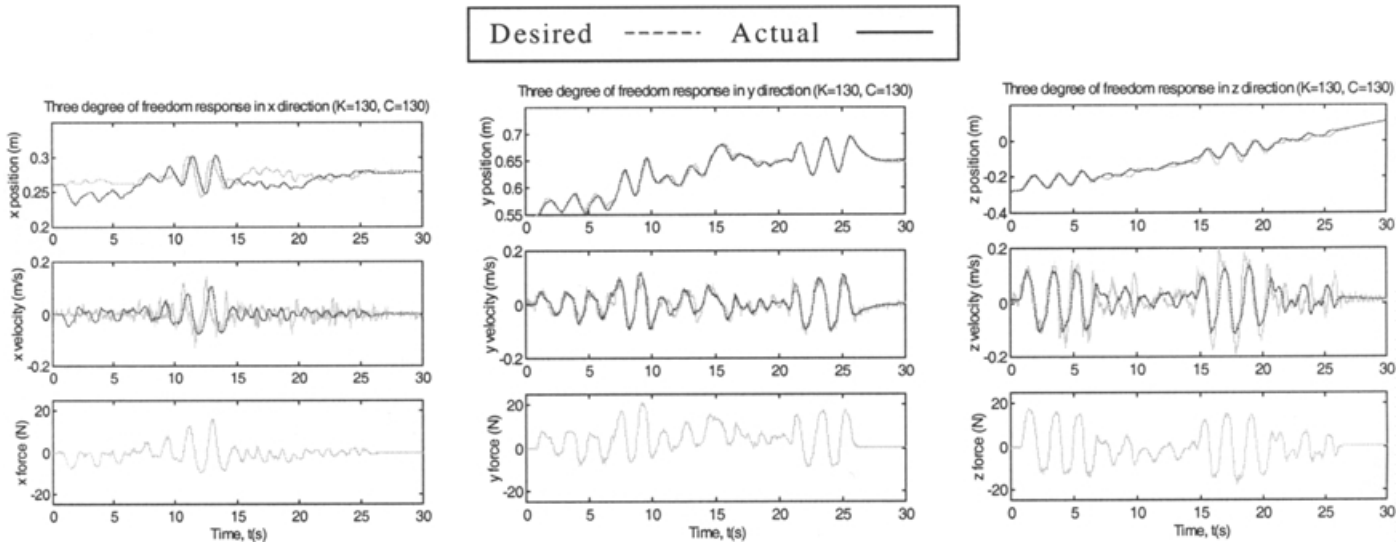

Fig. 26. Three degree-of-freedom impedance controller response (K = 130, C = 130).

performance when the impedance parameters are varied. Several factors affect the performance of the multiple degree-of-freedom controller such as the force sensor accuracy in multiple degrees of freedom, delays in response, the accuracy in resolving forces and robustness of the open-loop force controller. These factors manifest themselves by degrading the system response where high damping is required or large forces are applied.

4. ROBOTIC PHYSIOTHERAPY

The capability of the robot to modify its behaviour depending upon externally applied forces is crucial to administering physiotherapy. A conventional robot implementing purely position demands would simply drag the patients limb. Patients need to be given the chance to perform the exercise independently if they are capable, with forces being applied only if the patient experiences difficulty. The proposed exercise technique involves the patient attempting to follow a desired trajectory with visual feedback informing the patient the current and desired position.

Preliminary experiments were performed on two degrees of freedom of the three degree of freedom robot (locking joint 1 at zero degrees). Two degrees of freedom can be easily represented on a computer monitor providing clear visual feedback when performing the exercise. For the exercise a square is used to represent the desired robot endpoint position and a circle is used to represent the current robot position on the computer monitor (Figure 27). When little assistance is provided (low stiffness and damping) the robot end point can be freely moved, with little force applied by the robot to move its endpoint to the desired position. Note that if no external forces are applied

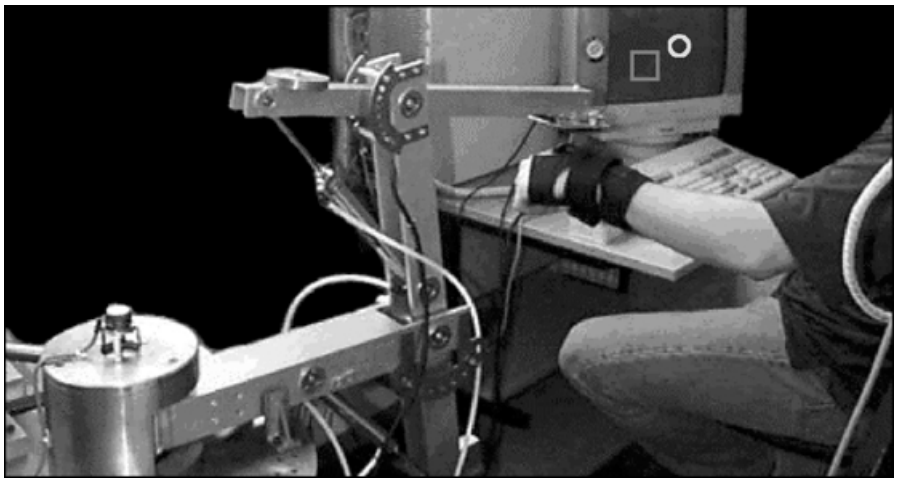

Fig. 27. Administering robot physiotherapy.

to the robot then it will still track the desired trajectory. When the assistance is increased the force the robot applies to move the end-point to the desired increases. Patients with low ability in their limb perform the exercise with high assistance. As they improve the assistance is reduced until they can perform the exercise without any assistance.

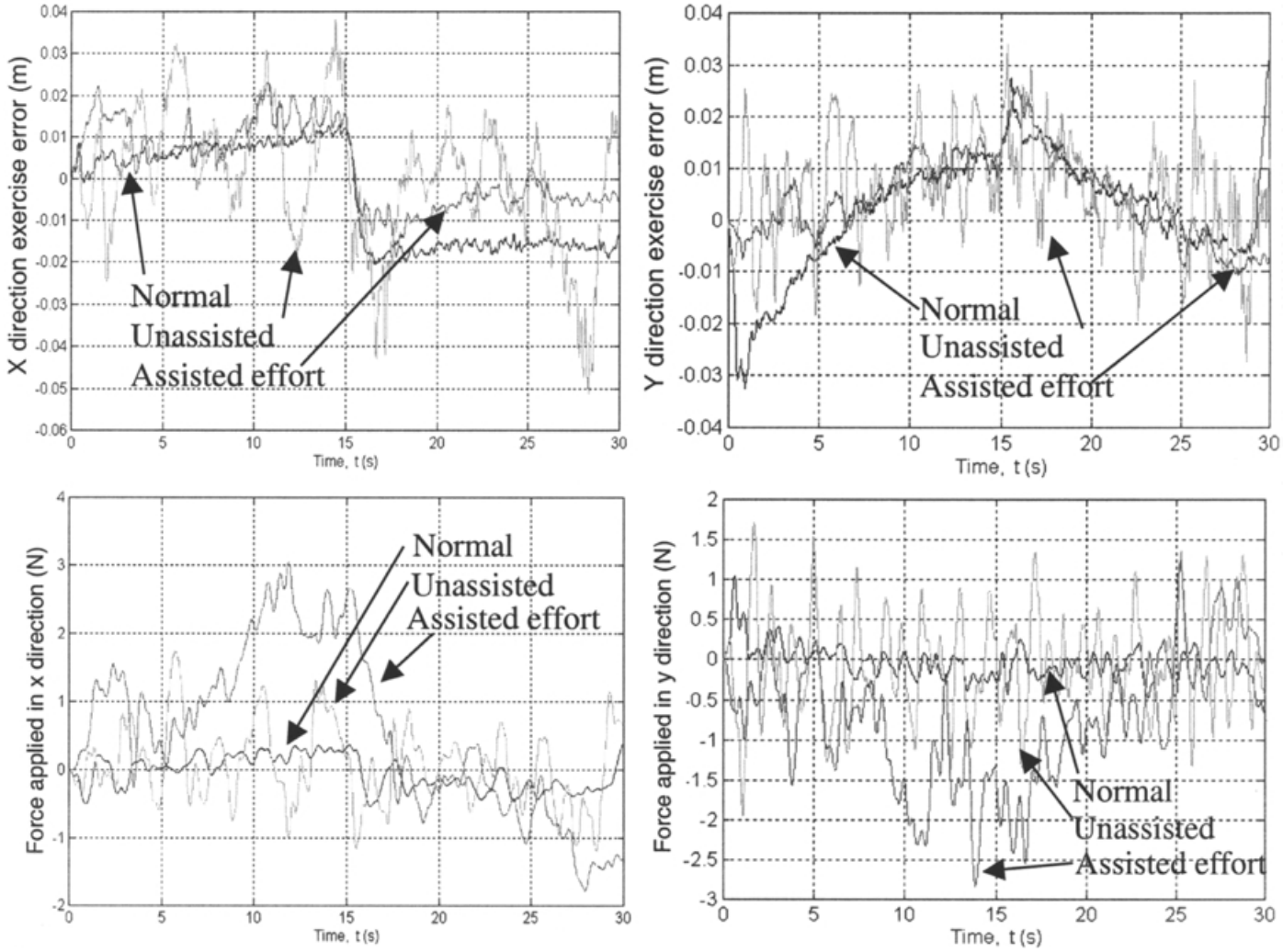

Fig. 28. Example physiotherapy results.

To evaluate the robot performance tests were performed on able-bodied subjects who were asked to perform the exercise three times; normal movement with low assistance, while performing a maximal task with their other arm and low assistance and a maximal task with high assistance. (A maximal task is one where a significant portion of brain function is given over to one task, reducing the ability of the brain to perform other functions such as the physiotherapy exercise.)

Example results of the robot performance are shown in Figure 28. In both directions of motion the exercise error (the error between the robot actual position and the desired position due to the impedance controller) is least for normal subject movement. Indicating the able-bodied subject has full use of their limb. Unassisted maximal effort results in greater exercise errors with the robot applying little force to correct the motion. The assisted maximal effort reduces the exercise errors by applying forces to the subject's motion that are apparent in the force traces. It should be noted that applying forces to this single point on a subject's arm could result in forces being applied to the vulnerable shoulder joint.

5. DISCUSSION AND CONCLUSIONS

A three degree-of-freedom robot has been designed and constructed that is capable of administering robotic physiotherapy. To measure interaction forces a three degree-of-freedom force sensor has been designed and fabricated. This sensor has been shown to measure force in multiple degrees of freedom, however it exhibits some cross coupling between orthogonally measured forces. The performance of the force sensor is critical to the performance of the control strategy.

Developments in pneumatics allow pneumatic actuators to be used in precision systems. As demonstrated here, they can be successfully used for precision applications. The quality of response of the pneumatic system has enabled the implementation of an impedance control strategy, initially on one degree of freedom and then multiple degrees of freedom. The performance on the single degree of freedom was very good, with the controller able to implement the full impedance control with mass, stiffness and damping and also the reduced controller within damping and stiffness only. The multiple degree of freedom controller performance was not as good as the single degree-of-freedom mainly due to errors in force measurement.

It was noted that the controller performance varies with the impedance characteristics specified. This is an important point and in characterising the performance of any impedance control strategy the performance across a range of impedance parameters must be considered.

The final robot has the potential to administer physiotherapy, however before any patient trials can be performed the quality of the force measurement needs to be improved. Further work will improve the controller performance and test the robot on a few sample patients.

References

1. J.M. Bamford, P. Sandercock, M. Dennis et al., "A prospective study of acute cerebrovascular disease in the community: the Oxfordshire Community Stroke Project 1981–1986: Methodology, demography,and incident cases of first ever stroke", *J. Neurol. Neurosurg. Psychiatry* **51**, 1373–1380 (1988).
2. G. Kwakkel, R.C. Wagenaar, J.W.R. Twisk et al., "Intensity of leg and arm training after primary middle cerebral artery stroke: a randomised controlled trial", *Lancet* **354**(9174), 191–196 (1999).
3. A. Sunderland, D.J. Tinson, E.L. Bradley et al., "Enhanced physical therapy improves recovery of arm function after stroke. A randomised controlled trial", *J. Neurol. Neurosurg. Psychiatry* **55**(7), 530–5 (1992).
4. P. Pound, C. Sabin and S. Ebrahim, "Observing the process of care: a stroke unit, elderly care unit and general medical ward compared", *Age and Ageing* **28**, 433–440 (1999).
5. J.A. Cozens, "Robotic assistance of an active upper limb exercise in neurologically impaired patients", *IEEE Trans. Rehabil. Eng.* **7**(2), 254–256 (1999).
6. H. Krebs, N. Hogan, M. Aisen and B. Volpe, "Robot-Aided Neurorehabilitation", *IEEE Transactions on Rehabilitation Engineering* **6**(1), 75–87 (1998).
7. M.A. Buckley, A. Yardley, R.G.S. Platts and S.S. Marchese, *MULOS system prototype* (Web page. http://www.ncl.ac.uk/crest/Prototype.htm#specification).
8. K. Nagai, I. Nakanishi and H. Hanafusa, "Development of an 8 DOF Robotic orthosis for assisting human upper limb motion", *Proceedings of the IEEE International Conference on Robotics and Automation* Belgium (1998) pp. 3486–3491.
9. M. H. Raibert and J. J. Craig, "Hybrid position/force control of manipulators", *ASME Journal of Dynamic Systems, Measurement and Control* **103**, 126–133 (1981).
10. S. Chiavervini and L. Sciavicco, "The parallel approach to force/position control of robotic manipulators", *IEEE Transactions on Robotics and Automation* **9**, No. 4, 361–373 (August, 1993).
11. N. Hogan, "Impedance control: An approach to manipulation part I, II, III", *Journal of Dynamic Systems, Measurements and Control* **107**(1), 1–24 (1985).
12. E. Richer and Y. Hurmuzlu. "High performance pneumatic force actuator system, Parts I & II", *Transactions of ASME* **122**, 416–425 (Sept., 2000).
13. J. Wang and Y. Y. Lin-Chen, "Modelling study, validation and robust tracking control of pneumatic cylinder actuator systems", *UKACC International Conference of Control 2000*, University of Cambridge (4–7 Sept., 2000).
14. R. Richardson, A. R. Plummer and M. D. Brown, "Self-tuning control of a low friction pneumatic actuator under the influence of gravity", *IEEE Transactions of Control Systems Technology* **9**, No. 2, 330–334 (March, 2001).
15. B. W. McDonell and J. E. Bobrow, "Modelling, identification and control of a pneumatically actuated robot", *Proceedings of the IEEE International Conference on Robotics and Automation* (April, 1997) pp. 124–129.
16. P. Gorce and M. Guihard, "Joint impedance pneumatic control for multilink systems", *ASME Journal of Dynamic Systems, Measurement and Control* **121**, 293–297 (June, 1999).
17. B. Heinrichs, N. Sepehri and A. B. Thorton-Trump, Position-based impedance control of an industrial hydraulic manipulator", *IEEE Control Systems Magazine* (special issue on robotics and automation) **17**, 46–52 (1997).
18. R. Richardson, M. D. Brown and A. R. Plummer, "Pneumatic impedance control for physiotherapy", *Proceedings of the EUREL Int. Conf. Robotics* (March, 2000).
19. R. Richardson, M. E. Austin and A. R. Plummer, "Development of a physiotherapy robot", *Proceedings of the International Biomechatronics Workshop*, Enshede (19–21 April, 1999).
20. E. J. McCormick, *Human Factors Engineering* (McGraw-Hill, Third edition, 1970).
21. S. Liu and J. E. Bobrow, "An analysis of a pnuematic servo system and it's application to a computer-controlled robot", *Transactions of ASME Journal of Dynamic Systems Measurements and Control* **110**, 228–235 (Sept., 1988).

22. G. Kim, D. Kang and S. Rhee, "Design and fabrication of a six-component force/moment sensor. Sensors and actuators", *Sensors and Actuators (A), physical* **77**, 209–220 (1999).
23. L. Chao and C. Yin, "The six-component force sensor for measuring the loading of the feet in locomotion", *Materials and Design* **20**, 237–244 (1999).
24. M. J. Fagan, *Finite Element Analysis* (Addison Wesley Longman, 1992, ISBN 0-582-02247-9).
25. R. C. Richardson, "Control and actuation for robotic physiotherapy", *PhD Thesis* (University of Leeds, UK, 2001).
26. W. H. Press, B. P. Flannery, S. Teukolosky and W. T. Verttering, *Numerical Recipes in C, the Art of Scientific Computing* (Cambridge University Press, 1991, ISBN 0-521-35465).
27. K. Astrom and T. Hagglund, *PID Controllers: Theory, Design and Tuning* (Instrument Society of America, 1994, ISBN 1-55617-516-7).
28. N. Hogan, "On the stability of manipulators performing contact tasks", *IEEE Journal of Robotics and Automation* **4**, 677–686 (1988).